ACADEMIC PRESS

Identification of novel enzyme–prodrug combinations for use in cytochrome P450-based gene therapy for cancer

Alex Baldwin, Zeqi Huang,[1] Youssef Jounaidi, and David J. Waxman[*]

Division of Cell and Molecular Biology, Department of Biology, Boston University, 5 Cummington St., Boston, MA 02215, USA

Abstract

Gene-directed enzyme prodrug therapy can be used to increase the therapeutic activity of anti-cancer prodrugs that undergo liver cytochrome P450 (CYP)-catalyzed prodrug to active drug conversion. The present report describes a cell-culture-based assay to identify CYP gene–CYP prodrug combinations that generate bystander cytotoxic metabolites and that may potentially be useful for CYP-based gene therapy for cancer. A panel of rat liver microsomes, comprising distinct subsets of drug-inducible hepatic CYPs, was evaluated for prodrug activation in a four-day 9L gliosarcoma cell growth inhibition assay. A strong NADPH- and liver microsome-dependent increase in 9L cytotoxicity was observed for the CYP prodrugs cyclophosphamide, ifosfamide, and methoxymorpholinyl doxorubicin (MMDX) but not with three other CYP prodrugs, procarbazine, dacarbazine, and tamoxifen. MMDX activation was potentiated $\sim$250-fold by liver microsomes from dexamethasone-induced rats (IC$_{50}$ (MMDX) $\sim$0.1 nM), suggesting that dexamethasone-inducible CYP3A enzymes contribute to activation of this novel anthracycline anti-tumor agent. This CYP3A dependence was verified in studies using liver microsomes from uninduced male and female rats and by using the CYP3A-selective inhibitors troleandomycin and ketoconazole. These findings highlight the advantages of using cell culture assays to identify novel CYP prodrug–CYP gene combinations that are characterized by production of cell-permeable, cytotoxic metabolites and that may potentially be incorporated into CYP-based gene therapies for cancer treatment.
© 2002 Elsevier Science (USA). All rights reserved.

Cytochrome P450 (CYP)[2] enzymes are endoplasmic reticulum-bound monooxygenases found in a variety of tissues, including the liver. These enzymes metabolize many lipophilic endogenous and xenobiotic substrates, including a large number of drugs and environmental chemicals [1,2]. The metabolism of drug substrates by CYP enzymes typically leads to drug inactivation and facilitates drug elimination. In some cases, however, CYP enzymes catalyze the activation of a comparatively nontoxic prodrug to form an active, cytotoxic drug metabolite. Examples of CYP prodrugs include the widely used anti-cancer alkylating agents cyclophosphamide (CPA) and ifosfamide (IFA) [3,4]. When activated in the liver, these anti-cancer CYP prodrugs are converted to reactive metabolites that circulate throughout the body and expose both tumor tissue and sensitive host cells to cytotoxic metabolites. A CYP-based prodrug activation strategy for cancer treatment has been introduced in an effort to increase therapeutic activity and reduce host toxicity associated with liver activation of these prodrugs [5,6]. The goal of this cancer gene therapy is to deliver a prodrug-activating CYP gene to cancer cells, enabling the formation of activated, cytotoxic metabolites directly within the tumor target, rather than in the liver. This may allow lower prodrug dosages to be employed, with correspondingly lower toxic side effects [7,8].

A significant problem with all gene therapy approaches, including CYP-based gene directed enzyme prodrug therapy (GDEPT), is the difficulty of achieving efficient expression of the therapeutic gene throughout

---

[*] Corresponding author. Fax: 1-617-353-7404.

E-mail address: djw@bu.edu (D.J. Waxman).

[1] Present address: GlaxoSmithKline, Research Triangle Park, NC 27502, USA.

[2] *Abbreviations used:* MMDX, 3′-deamino-3′-(2(S)-methoxy-4-morpholinyl); IFA, ifosfamide; CPA, cyclophosphamide; Dex, dexamethasone; BNF, β-naphthoflavone; PB, phenobarbital; TAO, troleandomycin (triacetyloleandomycin); GDEPT, gene-directed enzyme prodrug therapy; CYP, cytochrome P450; ER, estrogen receptor; Type II EBS, type II estrogen binding site; ddH$_2$O, distilled, deionized water.

the tumor. Tumor cells that do not express the therapeutic gene may escape the gene therapy and continue to proliferate. At present, no gene therapy vector or delivery method can ensure expression of a therapeutic gene in 100% of tumor cells in vivo [9]. One way to compensate for this limitation, in the case of GDEPT, lies in the selection of prodrugs that demonstrate a strong "bystander effect," whereby the activated prodrug readily diffuses from the tumor cell where it is formed into neighboring tumor cells, killing those cells even though they do not express the prodrug-activation gene [10].

The CYP prodrugs, CPA and IFA, are activated by a 4-hydroxylation reaction catalyzed by the human P450 enzyme CYP2B6 and by the rat P450 enzyme CYP2B1 [11,12]. The primary 4-hydroxy metabolite spontaneously decomposes into two reactive metabolites, the protein-binding metabolite acrolein and a DNA-alkylating phosphoramide mustard [3]. Rat 9L gliosarcoma cells that express CYP2B1 or CYP2B6 are highly sensitive to the cytotoxic effects of CPA. When treated with CPA, these CYP-expressing tumor cells generate cytotoxic metabolites characterized by a long-range bystander effect in vitro, killing neighboring, CYP-deficient tumor cells, both those in direct contact with the CYP 'factory cell' and more distant tumor cells as well [6,13]. IFA, an isomer of CPA with its own unique spectrum of anti-tumor activity, can also be activated by tumor-cell-expressed CYP2B enzymes, albeit somewhat less efficiently than CPA [13,14]. In contrast, the combination of herpes simplex virus–thymidine kinase with ganciclovir, widely studied as a GDEPT model system [15,16], shows a bystander effect that is more limited and primarily kills cells in direct contact with the thymidine kinase-expressing tumor cell [9].

Several other anti-cancer CYP prodrugs are known; however, their potential for successful incorporation into a CYP GDEPT strategy is largely unexplored [8]. When activated by CYP enzymes, the prodrugs procarbazine and dacarbazine both induce DNA methylation. Procarbazine activation can be catalyzed by certain CYP1A and CYP2B enzymes [17,18], while dacarbazine is activated by CYP1A and CYP2E enzymes [19,20]. The estrogen receptor (ER) antagonist tamoxifen is metabolized to a genotoxic metabolite by human CYPs 2B6, 2E1, and 3A4 in vitro [21]. Activated CYP metabolites of tamoxifen include 4-hydroxytamoxifen [22], which has a higher affinity for ER than tamoxifen alone [23,24], and various reactive metabolites that bind covalently to protein or DNA [25,26]. MMDX is a methoxymorpholinyl derivative of doxorubicin and is an inhibitor of both topoisomerases I and II [27]. Following incubation with liver microsomes, MMDX is metabolized to a DNA-alkylating cross-linker having 50-fold greater cytotoxic potential than the parent, prodrug form [28]. Recent work has demonstrated that MMDX activation is catalyzed by a
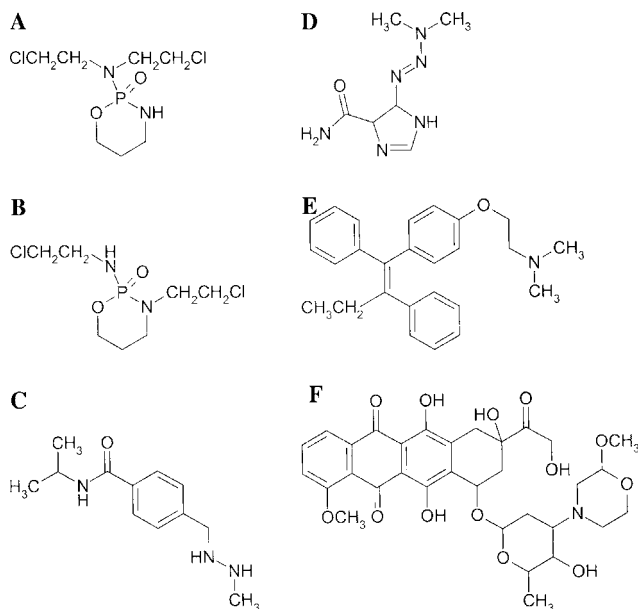

Fig. 1. Structure of CYP prodrugs. A, Cyclophosphamide; B, ifosfamide; C, procarbazine; D, dacarbazine; E, tamoxifen; F, MMDX.

CYP3A enzyme [29]. MMDX is currently undergoing phase II clinical trials [30] and shows great promise in circumventing resistance to doxorubicin, the parental compound, mediated by the drug exporter MDR-1 [27]. MMDX is more lipophilic than doxorubicin, which facilitates drug uptake by cells and may in part explain the ability of MMDX to kill tumor cells able to pump out doxorubicin [28].

The present study was carried out to evaluate novel prodrug–enzyme combinations that may potentially be suitable for use in CYP gene therapy. A modified metabolic activation assay [31] was used to evaluate the established anti-cancer prodrugs CPA and IFA, as well as four less well understood CYP prodrugs: procarbazine, dacarbazine, tamoxifen, and MMDX (Fig. 1). CYP prodrug activation was evaluated in a cell culture growth inhibition assay composed of rat 9L gliosarcoma cells incubated with drug in the presence of NADPH and liver microsomes from either uninduced or drug-induced rats, a readily available source rich in well-defined subsets of liver CYP enzymes. Our findings demonstrate the utility of this approach for identification of CYP prodrug–CYP gene combinations characterized by the formation of cell-permeable, cytotoxic metabolites likely to be associated with significant bystander cytotoxic potential.

Materials and methods

Chemicals

CPA (Cat#C0768), dacarbazine (Cat#D2390), NADPH (Cat#N6505), and troleandomycin (TAO)

(Cat#T6514) were purchased from Sigma–Aldrich (St. Louis, MO). IFA was obtained from the Drug Synthesis and Chemistry Branch, National Cancer Institute (Bethesda, MD). MMDX-HCl (PNU-152243) was a gift from Pharmacia & Upjohn (Milan, Italy). Procarbazine (Cat#P6858) and tamoxifen (Cat#T0250) were purchased from LKT Laboratories (St. Paul, MN). Ketoconazole (Cat#30.152.82) was obtained from Research Diagnostics (Flanders, NJ). Dacarbazine, procarbazine, and tamoxifen were stored dessicated at 4 °C. MMDX, CPA, IFA, and NADPH were stored dessicated at −20 °C. TAO and ketoconazole were stored in the dark at room temperature. CPA and IFA were prepared fresh as 100 mM stocks in distilled, deionized water (ddH$_2$O) (27.9 mg/ml CPA, 26.1 mg/ml IFA) prior to each experiment. Procarbazine (5 mM; 1.29 mg/ml) and dacarbazine (5 mM; 0.91 mg/ml) were prepared fresh for each experiment in sterile 15-ml tubes (Greiner Bio-One, Germany; Cat#188.271) by dissolving the compounds in culture medium with 10% FBS to give the desired final drug concentration. Dacarbazine could not be dissolved in either ddH$_2$O or DMSO at concentrations higher than ∼10 mM. Tamoxifen was dissolved in DMSO prior to each experiment at a stock concentration of 50 mM (28.2 mg/ml). MMDX was prepared as a 10 mM stock in ddH$_2$O (6.8 mg/ml) and then diluted to 10 μM and frozen in aliquots (activity was retained for >1 month at −20 °C). NADPH for use in microsome incubation experiments was prepared fresh for each experiment (120 mM; 99.96 mg/ml ddH$_2$O) and kept on ice until used. Stock solutions of 10 mM TAO (8.14 mg/ml) and 3 mM ketoconazole (1.6 mg/ml) were prepared in DMSO. Aliquots were stored at −20 °C for up to 1 month. Except for the initial weighing-out of chemicals, all preparation of chemicals was carried out under sterile conditions and in sterile tubes. This precaution was found to be sufficient to avoid cell culture contamination. Compounds dissolved in aqueous buffers (with the exception of compounds dissolved in culture medium containing FBS) were filtered–sterilized immediately following preparation using a 0.22-μm syringe filter (Pall Corporation, East Hills, NY; Cat#4454).

Liver microsomes

Liver microsomes from drug-induced and untreated (uninduced) Sprague–Dawley rats (20 mg/ml stocks) were purchased from In Vitro Technologies (Baltimore, MD), except as noted. Aliquots were prepared and stored at −80 °C. The liver microsomes used in these studies (In Vitro Technologies product numbers as indicated) were from uninduced (M00001), phenobarbital-induced (M70001), β-naphthoflavone-induced (M200001), and dexamethasone-induced (M40001) male rats and uninduced female (F00001) rats. Liver microsomes used for the CPA/IFA experiment in Fig. 3

were prepared in this laboratory by differential centrifugation using standard methods [11]. Procedures involving animals were carried out with approval of the institutional animal care and use committee at Boston University.

9L cells

The nitrosourea-induced rat gliosarcoma cell line 9L [32] is a brain-tumor-derived adherent cell line and was cultured in DMEM (pH 7.4) (Gibco–BRL Life Technologies, Rockville, MD) containing 10% fetal bovine serum (FBS) and a 1:100 dilution of concentrated penicillin/streptomycin antibiotic mixture (Gibco). Cells were cultured at 37 °C in a humidified incubator containing a 95% air, 5% CO$_2$ atmosphere. The 9L cells divide rapidly, and cell stocks maintained in 100-mm dishes were split 1:6 or 1:8 every 3–4 days. The 9L cells exhibit little density-based growth inhibition and once a confluent monolayer forms, cells begin to overgrow one another. At that point, sheets of cells detach easily during washes, preventing an accurate assessment of relative cell number. Cells growing in stock 100-mm dishes were treated for 6 min with 5 ml of trypsin (Gibco) diluted 1:10 with PBS. The trypsin–PBS solution was pipetted up and down repeatedly to detach the cells from the dish, following which the cells were transferred to a 15-ml Falcon tube containing 2.5 ml of DMEM with 10% FBS. The tubes were centrifuged at 1000 rpm for 5 min in a Sorvall RT 6000D centrifuge to pellet the suspended cells. The supernatant was then removed by aspiration and the cells were resuspended in fresh medium to give the desired concentration. Reattachment of cells was complete within 24 h.

Microsome–prodrug co-culture assay

The 9L cells were seeded in 96-well tissue culture microplates (Greiner Labortechnik, Germany; Cat#655180) at a density of 1000 cells/well, unless indicated otherwise, and allowed to attach for 24 h. The top row of each plate remained empty as a cell-free crystal violet stain negative control. Increasing concentrations of prodrug diluted in DMEM with 10% FBS were then added to each well, with the top two rows (the blank row and the first row with cells) containing no drug. Each prodrug concentration/microsome combination was assayed in triplicate wells. NADPH (0.3 mM) and (where present) 2 μg of rat liver microsomes were added to each well. The final volume of each well was adjusted to 200 μl with DMEM containing 10% FBS. Cells were routinely cultured for 4 days after the addition of prodrug. The culture medium was then removed and the wells were washed by gently adding 400 μl PBS along the side of each well to avoid disturbing the cells. Crystal

violet staining mixture (100 μl; stain composed of 1.25 g crystal violet, 50 ml of 37% formaldehyde, and 450 ml of methanol, stored at room temperature) [13] was added to each well and the plates were gently shaken for 20 min on an orbital shaker. Excess stain was removed using an 8-channel multipipette and the plates were washed twice by immersion in several liters of water at room temperature. The plates were then air-dried for 24 h. The cell-adhering crystal violet stain was then resuspended in 100 μl of 70% ethanol over a 20-min period with gentle shaking. A_{595} values (means ± SD for triplicate wells) were determined using an SLT SPECTRA Shell Reader (SLT Lab Instruments, Austria). A_{595} values for triplicate cell-free wells of each microsome type were subtracted from the average A_{595} at each prodrug concentration to adjust for background staining due to residual microsomal protein, FBS in the culture medium, and/or stain bound to the plastic plates. Data are expressed in the individual figures as relative growth rate at each drug concentration (with error bars representing standard deviation), determined by dividing the A_{595} value for a given prodrug concentration by the A_{595} of the drug-free control. A value of 1 corresponds to 100% cell growth rate, relative to the drug-free control. Trends presented in each figure are representative of two or three independent experiments; graphs shown and IC_{50} values mentioned in the text are based on single experiments deemed most representative. To determine the IC_{50} for a given liver microsome–prodrug combination, the relative cell growth vs the log of prodrug concentration was graphed. A computer-derived curve fit of the data (generated using the software package Cricket Graph 3) was generated. The slope equation was solved for the prodrug concentration corresponding to 50% growth inhibition.

Inhibitor experiments

9L microsome–prodrug co-culture assays were carried out in 96-well plates as described above but in the presence of increasing concentrations of either TAO or ketoconazole, as specified. TAO and ketoconazole stock solutions were diluted by dropwise addition to culture medium to achieve the desired final inhibitor concentration. The diluted inhibitor solutions were mixed thoroughly before addition to the cell culture plates to avoid precipitation seen when the inhibitor concentrations exceeded 200 μM (TAO) or 20 μM (ketoconazole), respectively. Cells were cultured for 4 days and then washed and stained with crystal violet as described above. Triplicate wells were averaged and background subtracted as above. To normalize the resulting A_{595} values to relative cell growth, the A_{595} of each microsome type/inhibitor concentration data point was divided by the A_{595} of the corresponding prodrug-free point.

Results

Evaluation of microsome–prodrug activation using a growth inhibition assay

Evaluation of microsomal CYP–prodrug combinations for potential use in prodrug-activation-based cancer gene therapy was carried out using 9L rat gliosarcoma cells grown in 96-well tissue culture plates. In an initial study, 9L cells were seeded at 0, 250, 450, and 1000 cells/well and allowed to grow for 3, 4, 5, or 6 days, followed by staining with crystal violet. Cell growth was essentially linear over all time points for all cell densities (Fig. 2). The A_{595} of the stained 1000-cell/well density plate was ~1.5 after 4 days of growth; these cell plating and growth conditions were selected for use in all subsequent 9L cell line 96-well cell culture assays. Microsome–prodrug co-culture assays were designed such that each well contained NADPH, prodrug, and liver microsomes isolated from either uninduced or drug-induced rats. Microsomes isolated from drug-induced rat liver were first tested for their ability to activate the established CYP prodrugs CPA and IFA. After a 4-day incubation of the cells with prodrug and liver microsomes, the cells were stained with crystal violet and the relative cell number quantitated (A_{595}) after subtraction of background staining (microsomal protein in the absence of cells).

CPA and IFA were activated to cytotoxic metabolites as revealed by the substantial decrease in 9L cell growth rate in cultures containing liver microsomes from phe-
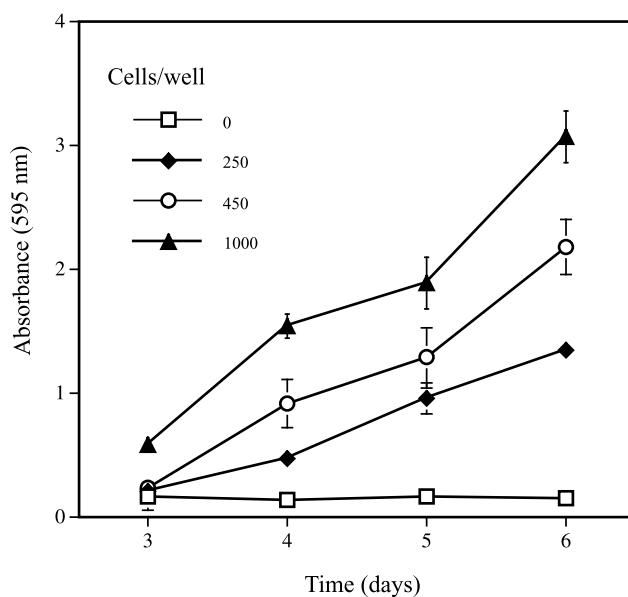

Fig. 2. 9L cell growth rate is linear from 3 to 6 days over a range of plated cell densities. Cells were seeded at 0, 250, 450, and 1000 cells/well in replicate plates and stained at 3, 4, 5, or 6 days as described in Materials and methods. Data shown are relative A_{595} values (crystal violet staining), means ± SD for $n = 6$ replicates.

nobarbital-induced rats (1 μg/well) (Fig. 3A). CPA (IC$_{50}$ ∼ 0.075 mM) was activated more efficiently than IFA (IC$_{50}$ ∼ 0.6 mM) by the induced microsomes. No significant cytotoxicity was observed in the absence of microsomes. These findings are consistent with the high catalytic activity of the phenobarbital-inducible
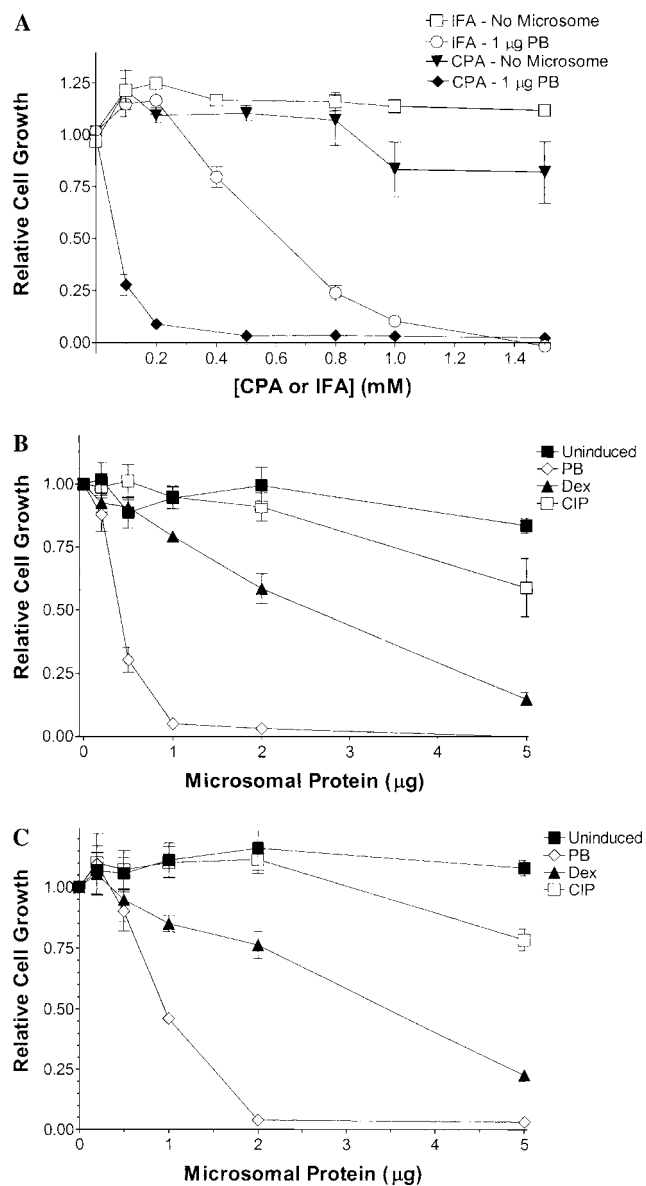

Fig. 3. Microsomal activation of CPA and IFA cytotoxicity by a panel of liver microsomes from drug-induced rats. The experiment was performed according to the standard 9L growth inhibition assay protocol described under Materials and methods, with minor alterations. (A) Prodrug (CPA or IFA) concentration was varied from 0 to 1.5 mM. Cells were cultured without microsomes (No Microsome) or with 1 μg of microsomes from phenobarbital-induced rats (1 μg PB). The activation of 0.5 mM CPA (B) or 0.5 mM IFA (C) is shown for a panel of liver microsomes over a range of microsomal protein concentrations. The panel included liver microsomes from uninduced, phenobarbital-induced (PB), dexamethasone-induced (Dex), and ciprofibrate-induced (CIP) male rats. Data shown are means ± SD values for n = 3 replicates.

CYP2B1 with both CPA and IFA as substrates [11,33]. Examination of microsomes from dexamethasone- and ciprofibrate-induced rats revealed protein-dependent microsome increases in the activity of CPA (Fig. 3B) and IFA (Fig. 3C). These findings demonstrate the utility of the assay method and show that an extracellular source of CYP activity can enhance CYP prodrug cytotoxicity in a manner comparable to that obtained using CYP-expressing tumor cell lines [6,13].

In subsequent experiments, a commercial panel of rat liver microsomes (isolated from uninduced rats or from rats treated with phenobarbital, dexamethasone, or β-naphthoflavone) was used as the source of CYP activity for investigating other CYP–prodrug combinations. No apparent increase in 9L growth inhibition was observed with three of the CYP prodrugs tested (procarbazine, dacarbazine, and tamoxifen) when incubated in the presence of liver microsomes from drug-induced rats (Fig. 4). Procarbazine showed very modest toxicity even at concentrations as high as 5 mM, both in the absence and in the presence of microsomes (Fig. 4A). Dacarbazine exhibited linear concentration-dependent toxicity, with a 40% cell growth rate, relative to the dacarbazine-free control, at 5 mM dacarbazine and no effect of microsomes apparent (Fig. 4B). Tamoxifen (Fig. 4C) was relatively nontoxic at 8 μM, but at 16 μM 100% cell growth inhibition was observed. No microsome-dependent increase in tamoxifen activity was observed. By contrast, strong microsome-dependent prodrug activation was seen with a fourth prodrug, MMDX (see Fig. 5, below). The absence of a microsome-dependent increase in cytotoxicity with the three CYP prodrugs shown in Fig. 4 may reflect a number of factors, including the absence of the relevant CYP enzyme activity in the microsomes tested and the formation of a reactive, short-lived prodrug metabolite with poor bystander activity (see Discussion).

Characterization of microsome-dependent MMDX activity

In the absence of liver microsomes, MMDX (10 nM) showed little toxicity to 9L cells. By contrast, a substantial increase in MMDX toxicity was observed in the presence of liver microsomes (Fig. 5A). The increase in MMDX toxicity was greatest with microsomes from dexamethasone-induced rats, followed by those from phenobarbital-induced rats. Liver microsomes from uninduced and β-naphthoflavone-induced rats also activated MMDX when compared to no microsome controls, albeit to a lesser degree than the microsomes from dexamethasone- and phenobarbital-induced rats.

Further investigation showed that MMDX is a highly potent, microsome-activated cytotoxic agent that is characterized by an IC$_{50}$ (MMDX) = 0.13 nM in the presence of liver microsomes from dexamethasone-
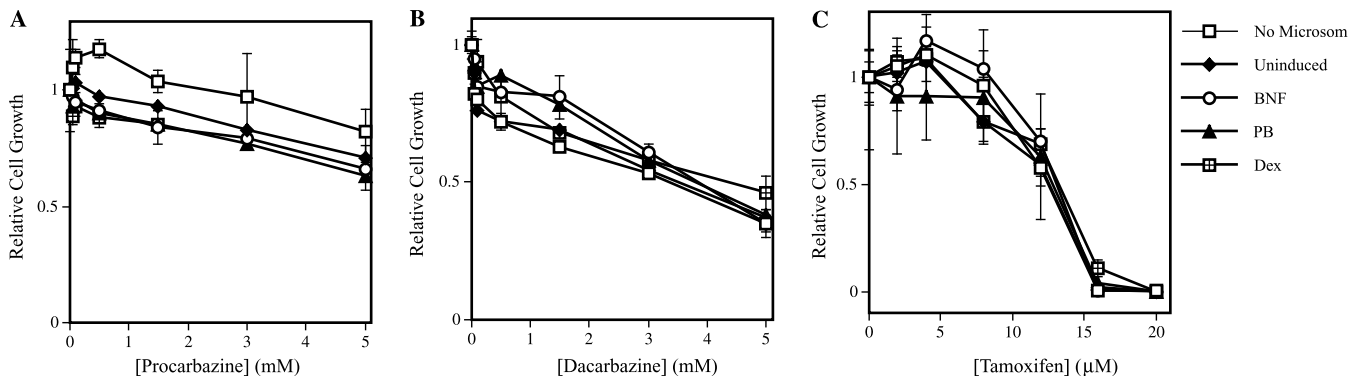
Fig. 4. Procarbazine, dacarbazine, and tamoxifen are not activated by rat liver microsomes. Procarbazine (A), dacarbazine (B), and tamoxifen (C) were cultured with 9L cells in the presence of NADPH and 2 µg of liver microsomes from uninduced or drug-induced rats as indicated. After 4 days, the plates were stained and quantitated as described under Materials and methods. Results are expressed as relative cell growth rates at each concentration of prodrug compared with the drug-free control (mean ± SD, $n = 3$ replicates). Panel members include no microsome (No Microsome) and liver microsomes from uninduced (Uninduced), β-naphthoflavone-induced (BNF), phenobarbital-induced (PB), and dexamethasone-induced (Dex) male rats.
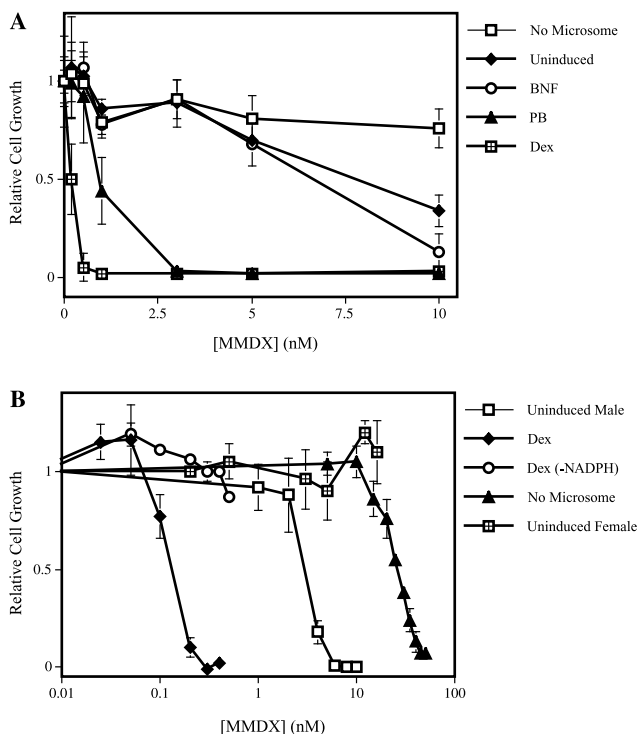

Fig. 5. Activation of MMDX by rat liver microsomes. (A) 9L cells were cultured for 4 days with MMDX, NADPH, and 2 µg of liver microsomes from uninduced or drug-induced rats, as indicated, at which time the plates were stained and relative cell growth rates determined as described in Materials and methods and Fig. 4. (B) Liver microsome-dependent MMDX activation was assayed as in panel A over the following ranges of MMDX concentrations: liver microsomes from uninduced male rats (Male, 0–10 nM MMDX); from dexamethasone-induced male rats (Dex, 0–0.5 nM MMDX); from dexamethasone-induced male rats in the absence of 0.3 mM NADPH (Dex (-NADPH), 0–0.5 nM MMDX); in the absence of liver microsomes (No Microsomes, 0–50 nM MMDX); and from uninduced female rats (Female, 0–16 nM MMDX). Log MMDX concentrations are graphed in panel B. IC_{50} (MMDX) values determined based on these data were 0.13, 2.6, and 25 nM for microsomes from dexamethasone-induced male rats, microsomes from uninduced male rats, and no microsomes, respectively. Data shown are means ± SD values for $n = 3$ replicates.

induced rats (2 µg protein/200 µl culture medium) in a standard 4-day 9L cell culture assay (Fig. 5B). This value can be compared to an IC_{50} of 2.6 nM for MMDX with liver microsomes from uninduced male rats and an $IC_{50} \sim 25$ nM in the absence of liver microsomes. No significant dexamethasone microsome-dependent increase in MMDX toxicity was observed in the absence of NADPH (Fig. 5B).

To investigate the possible role of dexamethasone-inducible CYP3A enzyme(s) in MMDX activation, we assayed the activity of liver microsomes from uninduced female rats, which contain low basal levels of several CYP3A enzymes [34]. At the prodrug concentrations tested (0–16 nM), microsomes from uninduced female rats exhibit a cytotoxic profile indistinguishable from that of the no-microsome controls (Fig. 5B).

In further experiments, the CYP3A-selective inhibitors TAO and ketoconazole were used to probe the role of CYP3A enzymes in MMDX activation. The macrolide antibiotic TAO is a highly selective CYP3A inhibitor [35]. TAO is metabolized by CYP3A to form a metabolite inhibitor complex with the CYP's heme group [36]. TAO at a concentration of 2 µM substantially blocked the uninduced male rat liver microsome-dependent activation of MMDX (5 nM and 10 nM; Fig. 6A). TAO also blocked activation of MMDX (0.5 nM and 1 nM) by microsomes from dexamethasone-induced rats in a TAO concentration-dependent manner (Fig. 6A), although with 1 nM MMDX and microsomes from dexamethasone-induced rats the inhibition was incomplete, even at 75 µM TAO (Fig. 6A).

Ketoconazole is a potent ($IC_{50} \sim 0.3$ µM) CYP3A inhibitor, albeit with lower selectivity than TAO, as indicated by the inhibition of other CYP enzymes seen at high ketoconazole concentrations (cf. $IC_{50} \sim 15$ µM for the human enzyme CYP2C8) [37]. Low concentrations of ketoconazole (1 µM) completely inhibited MMDX
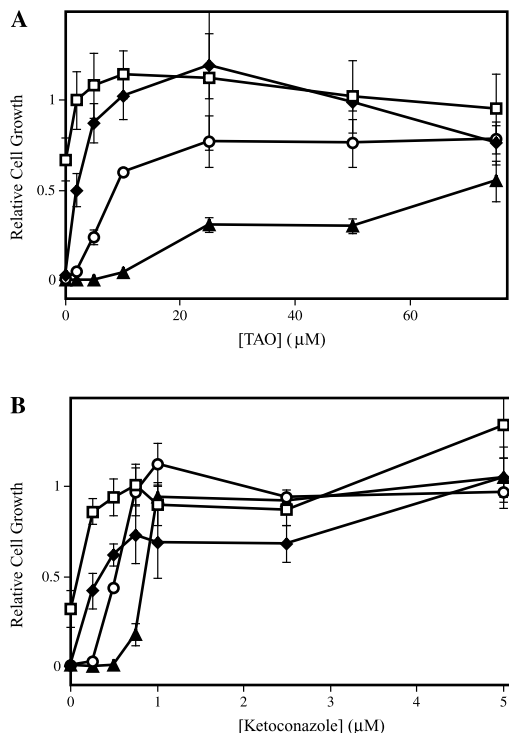
Fig. 6. Inhibition of liver microsomal MMDX activation by TAO and ketoconazole. Assays were carried out as in Fig. 5 in the presence of NADPH (0.3 mM) and the indicated concentrations of MMDX (0.5 or 1 nM MMDX for microsomes from dexamethasone-induced rats (open circles and closed triangles, respectively), and 5 or 10 nM MMDX for microsomes from uninduced male rats (open squares and closed diamonds, respectively)). Each inhibitor was included in the culture medium as specified, 0–75 μM for TAO (A) and 0–5 μM for ketoconazole (B). After 4 days, the plates were stained and quantitated as described under Materials and methods. Data shown are means ± SD values for $n = 3$ replicates.

activation catalyzed by liver microsomes isolated from uninduced and dexamethasone-induced male rats (Fig. 6B). As was observed with TAO, the concentration of ketoconazole needed to fully inhibit MMDX activation was highest with microsomes from dexamethasone-induced rats and at higher MMDX concentrations. Taken together, these experiments strongly support the proposed role of CYP3A in MMDX activation.

Discussion

A new generation of treatment strategies is currently being developed to improve the efficacy and reduce the side effects of cancer chemotherapy. One such strategy is cytochrome P450-based prodrug activation gene therapy for cancer treatment [8]. By the delivery of a prodrug-activating CYP gene directly to a tumor, the tumor acquires the capacity for prodrug activation, enabling the localized production of cytotoxic CYP-activated prodrug metabolites. This approach may decrease systemic exposure to cytotoxic metabolites, potentially allowing increased efficacy at lower prodrug doses, with a corresponding decrease in toxicity to sensitive host tissues. This gene-based therapy can be combined with localized delivery of the chemotherapeutic agent, as shown by the use of prodrug-impregnated polymer implants to further increase efficacy and decrease systemic drug exposure [38]. Several established chemotherapeutic prodrugs are activated via CYP-catalyzed reactions, including CPA, IFA, procarbazine, and dacarbazine [39,40]. However, with the exception of CPA and IFA, the potential utility of these prodrugs for CYP GDEPT is largely unexplored. The aim of the present study was to develop a tumor cell culture-based assay to identify CYP enzyme–CYP prodrug combinations that may be suitable for use in CYP-based gene therapy.

Assay for CYP-activated anti-cancer prodrugs

In the assay described here, 9L gliosarcoma cells were cultured in the presence of rat liver microsomes, NADPH, and a potential CYP prodrug. Rat liver microsomes are well suited as the source of liver P450 activity for this assay, as they are composed of well-defined subsets of CYP enzymes that can be highly induced by treating rats with classical CYP-inducing agents, such as dexamethasone and phenobarbital [41]. Moreover, the extent to which a CYP prodrug is activated by a given preparation of drug-induced liver microsomes provides an initial indication of which CYP enzyme(s) activate the prodrug of interest. By carrying out the assay in 96-well tissue culture plates, large number of prodrugs can be assayed in parallel across a panel of liver microsomes from uninduced and drug-induced rats to identify the most active microsome–prodrug combinations. Furthermore, the addition of liver microsomes directly to the culture medium makes this assay suitable for screening tumor cell lines to identify specific cell lines and tumor cell types that are particularly sensitive to a given prodrug, without the need to transfect each cell line with a prodrug-activating CYP cDNA. Moreover, because the metabolites generated using this assay are already external to the cells, any finding of microsome-dependent cytotoxicity provides good evidence that the activated drug is sufficiently long-lived to penetrate the cell membrane and gain access to its intracellular target and site of action. CYP–prodrug combinations identified in this manner are thus likely to exhibit the desired bystander cytotoxic effect. Present gene therapy vectors are incapable of transducing the cells of a tumor with 100% efficiency; thus, it is essential that cytotoxic metabolites generated within a tumor cell be soluble, diffusible, and sufficiently long-lived so that they can enter and kill neighboring tumor cells that do not express the prodrug-activating enzyme. The ability to screen for CYP–prodrug combinations

that have this bystander potential is an important feature of the present assay method.

The assay described here lends itself to high-throughput analysis of libraries of compounds to identify previously unknown CYP prodrugs. The assay may also be adapted for use with panels of microsomes composed of single cDNA-expressed human or rodent CYP enzymes, which are widely available from commercial sources (e.g., BD-Gentest Supersomes). Use of the latter microsomes provides the added advantage of a more precise definition of the specific CYPs (rat and human) that exhibit the highest potential for activation of the prodrug of interest, which in turn may facilitate the selection of optimal CYP genes for further evaluation in prodrug activation gene therapy. Single enzyme-enriched, cDNA-expressed microsomes would also more accurately reflect the ultimate gene-therapy regimen, wherein a single CYP gene would be expressed in the target tumor. Finally, application of this approach to the National Cancer Institute's panel of 60 human tumor cell lines currently used to screen for novel anti-cancer prodrugs [42] could facilitate the identification of novel CYP-activated prodrugs, insofar as the cell lines that compose that panel are largely devoid of CYP activity [43].

One potential limitation of this assay is the anticipated insensitivity of 9L cells to some CYP prodrugs, which would thus escape detection in the assay. Although 9L cells are not generally regarded as drug-resistant, they are unlikely to exhibit high intrinsic sensitivity to all CYP-activated prodrugs. This insensitivity could contribute to the inactivity of the CYP prodrugs procarbazine and dacarbazine seen in the present study. Accordingly, it may be useful to incorporate additional tumor cell lines into any CYP prodrug screen. Prodrugs that are not activated by the CYP enzymes present in the panel of liver microsomes used in the assay could also be missed. To address this problem, additional CYP-expressing microsomes, including microsomes containing single cDNA-expressed human CYPs, could be included in the panel to ensure that the relevant CYP enzyme activity is present. The growth inhibition assay could also be extended to longer times (cf. Fig. 2) to increase the sensitivity of the assay. Finally, not all human tumor cells will exhibit the CYP prodrug sensitivity profile of 9L cells for reasons relating to their intrinsic or acquired drug resistance. Follow-up studies would therefore be needed to establish the profile of human tumor cell line sensitivity to any CYP–prodrug combination identified using this approach.

Activation of CPA and IFA by liver microsomes from drug-induced rats

Liver microsomes from phenobarbital-induced rats and, to a lesser degree, from dexamethasone- and ciprofibrate-induced rats were able to activate CPA and IFA. The difference in the degree of activation of CPA by microsomes from rats induced with phenobarbital vs ciprofibrate (Fig. 2B) corresponds to the relative effectiveness of these agents as inducers of CYP2B1, which activates CPA by a 4-hydroxylation reaction [11]. In the case of IFA, 4-hydroxylation can be catalyzed by CYP2B1 (phenobarbital-inducible) or by CYP3A enzymes (inducible by phenobarbital or dexamethasone) [33,44]. However, the relatively strong activation of CPA currently seen with liver microsomes from dexamethasone-induced rats was unexpected, insofar as dexamethasone is a poor inducer of CYP2B1 activity, and dexamethasone-inducible CYP3A enzymes do not catalyze CPA 4-hydroxylation [11,44]. CYP3A enzymes do, however, catalyze CPA N-dechlorethylation, which produces chloroacetaldehyde as a by-product [44]. Although generally regarded as a neurotoxic agent without therapeutic value, chloroacetaldehyde does have a cytotoxic effect on tumor cells [45], which may contribute to the cytotoxicity of CPA in the present study seen with microsomes from dexamethasone-induced rats.

MMDX is activated by CYP3A enzymes

Significant liver microsome- and NADPH-dependent 9L cytotoxicity was observed with the doxorubicin derivative MMDX. MMDX was the most potent of the six CYP prodrugs tested, with an IC_{50} of $\sim 0.1\,nM$ in the presence of dexamethasone-induced liver microsomes and an IC_{50} of $\sim 25\,nM$ in the absence of liver microsomes. MMDX activation was also catalyzed by liver microsomes from uninduced male rats, albeit much less efficiently ($IC_{50} \sim 2.6\,nM$) compared to dexamethasone-induced microsomes, consistent with the lower CYP3A activity of liver microsomes from uninduced male rats [46]. The M5076 hepatic tumor cell line, previously employed to assay MMDX toxicity, may be less sensitive to MMDX than 9L cells, as indicated by the IC_{50} of $\sim 4\,nM$ observed using liver microsomes from rats induced with the CYP3A inducer pregnenolone-16α-carbonitrile [29]. Liver microsomes from uninduced female rats, which have an even lower CYP3A activity than those from uninduced male rats [46], were unable to activate MMDX in the present 9L cell culture assay. Further experiments showed that the CYP3A-selective inhibitors TAO and ketoconazole specifically inhibited liver-microsome-catalyzed MMDX activation, in accord with the role of CYP3A enzymes in MMDX activation proposed by Quintieri and colleagues in an earlier report [29]. The incomplete inhibition of dexamethasone-inducible microsomal MMDX activity seen with TAO suggests that MMDX may have a much lower K_d than TAO for binding to the dexamethasone-inducible microsomal CYP3A enzyme(s), a possibility that is in accord with the subnanomolar IC_{50} for MMDX activation exhibited by the dexamethasone-induced liver microsomes.

Conceivably, the extent of TAO inhibition may be increased by preincubating the liver microsomes with TAO prior to addition of MMDX to the culture medium.

Rat liver contains at least four distinct CYP3A enzymes that may potentially activate MMDX, CYPs 3A1, 3A2, 3A9, 3A18, in addition to CYP3A23, an allelic variation of CYP3A1 [34]. CYP3A2 is present at high levels in liver microsomes from uninduced male rats but is essentially undetectable in microsomes from uninduced females [34], suggesting that this CYP3A form plays a major role in microsome-catalyzed MMDX activation produced by liver microsomes from uninduced male rats. CYP3A2 is inducible by dexamethasone [34], suggesting that CYP3A2 may also contribute to the increased MMDX activity seen with microsomes from dexamethasone-induced rats, although to what degree remains unknown. In contrast, CYP3A9 is not induced by dexamethasone treatment and is expressed in uninduced female rat liver at twice the level present in males [34]. CYP3A9 is unlikely to metabolize MMDX, given the inactivity of liver microsomes from uninduced female rats in the 9L cell MMDX activation assays. CYP3A1 and CYP3A18 are both expressed at low levels in the liver microsomes of uninduced rats of both sexes and are highly inducible by dexamethasone [34]. Therefore, either (or both) of these CYP3A enzymes could contribute (along with CYP3A2) to the increased MMDX cytotoxicity seen with microsomes from dexamethasone-induced male rats. Further analysis using individual cDNA-expressed enzymes is required to fully elucidate the profile of rat and human CYP3A enzymes capable of activating MMDX.

Lack of liver-microsome-dependent activation of procarbazine, dacarbazine, and tamoxifen

Procarbazine and dacarbazine exhibited little cytotoxicity to 9L cells, even in the presence of liver microsomes and at concentrations of ~5 mM. In a previous study, in the absence of liver microsomes, no procarbazine cytotoxicity to L1210 leukemia cells was observed, even after 10 days of 1 mM drug treatment [47]. Liver CYP-catalyzed activation of procarbazine [17] and dacarbazine [20] has been demonstrated and is thought to involve CYP-generated alkyl radicals, which may be too short-lived and too highly reactive to cross cell membranes and exert significant cytotoxicity when they are formed extracellularly. Under such circumstances, no microsome-dependent cytotoxicity would be detectable in the present assay system, even if prodrug activation were occurring. Prodrugs that form short-lived, reactive metabolites would likely exhibit a poor bystander effect and would, therefore, not be particularly useful in a CYP-based GDEPT strategy.

Tamoxifen and its activated metabolite, 4-hydroxytamoxifen, are estrogen receptor (ER) antagonists, with 4-hydroxytamoxifen exhibiting a significantly higher affinity for the receptor than the parent drug [23]. In the case of ERα, tamoxifen and 4-hydroxytamoxifen can both bind to the receptor and elicit estrogenic and inhibitory effects, while their binding to ERβ is strictly inhibitory; however, the higher affinity of 4-hydroxytamoxifen compared to the parent prodrug is independent of the ER subtype [48]. In addition, a cell surface receptor, type II estrogen binding site (type II EBS), may also be a target of tamoxifen action, as it induces a growth inhibitory effect in the presence of tamoxifen similar to that seen in classical ER-positive cells ($IC_{50} \sim 0.1\,\mu M$) [49]. An ER-independent action of tamoxifen involving the inhibition of protein kinase C [50] is known but occurs at $15–100\,\mu M$ tamoxifen, well above the concentrations at which type II EBS/ER-dependent growth inhibition takes effect. In the present study, tamoxifen effected complete 9L cell growth inhibition at $16\,\mu M$ (Fig. 4C), making protein kinase C inhibition a plausible mechanism. Tamoxifen can also undergo alternate metabolic reactions, leading to the formation of metabolites such as N-desmethyl-tamoxifen, a nontherapeutic metabolite. This reaction is catalyzed by rat CYP3A enzymes [51] and could potentially decrease the availability of drug for activation by other CYP-dependent metabolic pathways.

In conclusion, the usefulness of a 9L cell culture-based assay for identifying potential CYP prodrugs has been demonstrated. The proven utility of 9L cells in CYP–prodrug activation gene therapy studies [6,13], in combination with this tumor cell line's rapid growth rate and capacity for growth as solid tumors when implanted either subcutaneously or intracranially, make this an ideal system, both for the initial characterization of CYP enzyme-CYP prodrug combinations shown here, and for subsequent in vivo gene therapy studies. The striking, 250-fold potentiation of MMDX cytotoxicity and the very low (subnanomolar) concentrations of MMDX required to induce tumor cell death in the presence of liver microsomes from dexamethasone-induced rats make MMDX a promising candidate for CYP-based GDEPT. IFA can also be activated by CYP3A enzymes, raising the possibility that MMDX might be used in combination with IFA in a multidrug GDEPT treatment. By enhancing cytotoxic activity, and by increasing the target cell specificity of drug exposure, CYP-based gene therapy holds out the promise of improved therapeutic efficacy for clinically established and investigational cancer chemotherapeutic CYP prodrugs.

encouragement that he has extended to young investigators in the field of cytochrome P450 for the past four decades.

References

[1] R.W. Estabrook, Science 160 (1968) 1368–1377.
[2] R.W. Estabrook, FASEB J. 10 (1996) 202–204.
[3] N.E. Sladek, Pharmacol. Ther. 37 (1988) 301–355.
[4] A.V. Boddy, S.M. Yule, Clin. Pharmacokinet. 38 (2000) 291–304.
[5] M.X. Wei, T. Tamiya, M. Chase, E.J. Boviatsis, T.K. Chang, N.W. Kowall, F.H. Hochberg, D.J. Waxman, X.O. Breakefield, E.A. Chiocca, Hum. Gene Ther. 5 (1994) 969–978.
[6] L. Chen, D.J. Waxman, Cancer Res. 55 (1995) 581–589.
[7] D.J. Waxman, L. Chen, J.E. Hecht, Y. Jounaidi, Drug Metab. Rev. 31 (1999) 503–522.
[8] L. Chen, D.J. Waxman, Curr. Pharm. Des. 8 (2002) 99–110.
[9] P.D. Wadhwa, S.P. Zielske, J.C. Roth, C.B. Ballas, J.E. Bowman, S.L. Gerson, Annu. Rev. Med. 53 (2002) 437–452.
[10] I.M. Pope, G.J. Poston, A.R. Kinsella, Eur. J. Cancer 33 (1997) 1005–1016.
[11] L. Clarke, D.J. Waxman, Cancer Res. 49 (1989) 2344–2350.
[12] T.K. Chang, G.F. Weber, C.L. Crespi, D.J. Waxman, Cancer Res. 53 (1993) 5629–5637.
[13] Y. Jounaidi, J.E. Hecht, D.J. Waxman, Cancer Res. 58 (1998) 4391–4401.
[14] P. Muller, R. Jesnowski, P. Karle, R. Renz, R. Saller, H. Stein, K. Puschel, K. von Rombs, H. Nizze, S. Liebe, T. Wagner, W.H. Gunzburg, B. Salmons, M. Lohr, Ann. N. Y. Acad. Sci. 880 (1999) 337–351.
[15] M. Caruso, Mol. Med. Today 2 (1996) 212–217.
[16] F.L. Moolten, Cancer Res. 46 (1986) 5276–5281.
[17] L. Goria-Gatti, A. Iannone, A. Tomasi, G. Poli, E. Albano, Carcinogenesis 13 (1992) 799–805.
[18] R.A. Prough, M.I. Brown, G.A. Dannan, F.P. Guengerich, Cancer Res. 44 (1984) 543–548.
[19] S. Yamagata, S. Ohmori, N. Suzuki, M. Yoshino, M. Hino, I. Ishii, M. Kitada, Drug Metab. Dispos. 26 (1998) 379–382.
[20] J.M. Reid, M.J. Kuffel, J.K. Miller, R. Rios, M.M. Ames, Clin. Cancer Res. 5 (1999) 2192–2197.
[21] J.A. Styles, A. Davies, C.K. Lim, F. De Matteis, L.A. Stanley, I.N. White, Z.X. Yuan, L.L. Smith, Carcinogenesis 15 (1994) 5–9.
[22] S.S. Dehal, D. Kupfer, Cancer Res. 57 (1997) 3402–3406.
[23] B.S. Katzenellenbogen, M.J. Norman, R.L. Eckert, S.W. Peltz, W.F. Mangel, Cancer Res. 44 (1984) 112–119.
[24] J.L. Borgna, H. Rochefort, J. Biol. Chem. 256 (1981) 859–868.
[25] S.S. Dehal, D. Kupfer, Drug Metab. Dispos. 27 (1999) 681–688.
[26] P.W. Fan, J.L. Bolton, Drug Metab. Dispos. 29 (2001) 891–896.
[27] G.E. Duran, D.H. Lau, A.D. Lewis, J.S. Kuhl, T.K. Bammler, B.I. Sikic, Cancer Chemother. Pharmacol. 38 (1996) 210–216.
[28] D.H. Lau, G.E. Duran, A.D. Lewis, B.I. Sikic, Br. J. Cancer 70 (1994) 79–84.
[29] L. Quintieri, A. Rosato, E. Napoli, F. Sola, C. Geroni, M. Floreani, P. Zanovello, Cancer Res. 60 (2000) 3232–3238.
[30] M. Bakker, J.P. Droz, A.R. Hanauske, J. Verweij, A.T. van Oosterom, H.J. Groen, M.A. Pacciarini, L. Domenigoni, F. van Weissenbruch, E. Pianezzola, E.G. de Vries, Br. J. Cancer 77 (1998) 139–146.
[31] J. Lebsanft, J.B. McMahon, G.G. Steinmann, R.H. Shoemaker, Biochem. Pharmacol. 38 (1989) 4477–4483.
[32] H.H. Schmidek, S.L. Nielsen, A.L. Schiller, J. Messer, J. Neurosurg. 34 (1971) 335–340.
[33] G.F. Weber, D.J. Waxman, Biochem. Pharmacol. 45 (1993) 1685–1694.
[34] A. Mahnke, D. Strotkamp, P.H. Roos, W.G. Hanstein, G.G. Chabot, P. Nef, Arch. Biochem. Biophys. 337 (1997) 62–68.
[35] T.K. Chang, F.J. Gonzalez, D.J. Waxman, Arch. Biochem. Biophys. 311 (1994) 437–442.
[36] M.R. Franklin, Methods Enzymol. 206 (1991) 559–573.
[37] M. Maurice, L. Pichard, M. Daujat, I. Fabre, H. Joyeux, J. Domergue, P. Maurel, FASEB J. 6 (1992) 752–758.
[38] T. Ichikawa, W.P. Petros, S.M. Ludeman, J. Fangmeier, F.H. Hochberg, O.M. Colvin, E.A. Chiocca, Cancer Res. 61 (2001) 864–868.
[39] K.T. Kivisto, H.K. Kroemer, M. Eichelbaum, Br. J. Clin. Pharmacol. 40 (1995) 523–530.
[40] G.A. Le Blanc, D.J. Waxman, Drug Metab. Rev. 20 (1989) 395–439.
[41] D.J. Waxman, L. Azaroff, Biochem. J. 281 (1992) 577–592.
[42] A. Monks, D. Scudiero, P. Skehan, R. Shoemaker, K. Paull, D. Vistica, C. Hose, J. Langley, P. Cronise, A. Vaigro-Wolff, M. Gray-Goodrich, H. Campbell, J. Mayo, M. Boyd, J. Natl. Cancer Inst. 83 (1991) 757–766.
[43] L.J. Yu, J. Matias, D.A. Scudiero, K.M. Hite, A. Monks, E.A. Sausville, D.J. Waxman, Drug Metab. Dispos. 29 (2001) 304–312.
[44] L. Yu, D.J. Waxman, Drug Metab. Dispos. 24 (1996) 1254–1262.
[45] K. Borner, J. Kisro, S.K. Bruggemann, W. Hagenah, S.O. Peters, T. Wagner, Drug Metab. Dispos. 28 (2000) 573–576.
[46] D.J. Waxman, G.A. Dannan, F.P. Guengerich, Biochemistry 24 (1985) 4409–4417.
[47] D.S. Swaffar, M.G. Horstman, J.Y. Jaw, B.D. Thrall, G.G. Meadows, W.G. Harker, G.S. Yost, Cancer Res. 49 (1989) 2442–2447.
[48] T. Barkhem, B. Carlsson, Y. Nilsson, E. Enmark, J. Gustafsson, S. Nilsson, Mol. Pharmacol. 54 (1998) 105–112.
[49] S. Caltagirone, F.O. Ranelletti, A. Rinelli, N. Maggiano, A. Colasante, P. Musiani, F.B. Aiello, M. Piantelli, Am. J. Respir. Cell Mol. Biol. 17 (1997) 51–59.
[50] H.D. Su, G.J. Mazzei, W.R. Vogler, J.F. Kuo, Biochem. Pharmacol. 34 (1985) 3649–3653.
[51] D. Kupfer, S.S. Dehal, Methods Enzymol. 272 (1996) 152–163.